DOUBLE-DIFFUSIVE NATURAL CONVECTION IN A CAVITY WITH AN INNER CYLINDER WRAPPED BY A POROUS LAYER

by

Mourad MODERRES[a*], Toufik BENMALEK[b], Aberkan SOFIANE[b], Abderrahmene GHEZAL[b], Said ABBOUDI[c], and Abderrahmene BENBRIK[d]

[a] Laboratory of Fluids Industries, Measures and Applications (FIMA) UDBKM, Ain Defla, Algeria
[b] Laboratory of Mechanical and Applied Fluids, USTHB, B.P.32, El-Alia, Bab-Ezzouar, Algiers, Algeria
[c] Interdisciplinary Laboratory Carnot de Bourgogne ICB UMR 6303 CNRS - UTBM Site (UBFC), Belfort Cedex, France
[d] Laboratory of Petroleum Equipements Reliability and Materials, UMBB, Boumerdes, Algeria

Original scientific paper
https://doi.org/10.2298/TSCI201112202M

This paper reports a numerical study of double-diffusive natural convection through an annular space delimited by a square cylinder on the outside and a cylindrical cylinder on the inside covered by a porous layer. The Darcy-Brinkmann-Forchheimer is used for modeling flow in both fluid and porous areas. The annular space is partially or completely filled with an isotropic porous medium. A finite volume method, using the Patankar-Spalding technique is used for solving the discretization of the dimensionless equations governing the problem. The effects of simultaneously applied thermal and solutal buoyancy forces on heat and mass transfer are shown in the results for a large range of buoyancy ratios, Rayleigh number, and thermal conductivity. Streamlines, isotherms, and iso-concentrations are presented to analyze the flow structure transition from mass species dominated to thermal dominated flow. Results show that the buoyancy ratio can change the flow pattern and the increased thermal conductivity ratio can improve heat and mass transfer. A good agreement was obtained between the present results and those published were found.

Key words: *natural convection, buoyancy ratio, double-diffusive convection, porous layer, heat and mass transfer*

Introduction

The phenomenon of natural convection through the porous medium has been investigated widely in the past Combarnous *et al.* [1] and the book of Nield *et al.* [2]. Natural convection in annular space with a porous medium has long been a subject of interest due to their wide engineering and technology applications such as in solar collector-receivers, Valipour *et al.* [3], thermal storage, petrochemical processes, fuel cells, cooling of electronic equipment, cooling system in nuclear reactors and metal solidification processes Yang and Ma [4] and Vijaya Venkata Raman *et al.* [5]. Double-diffusive convection flow caused by the combined influence of temperature and concentration gradients with a porous medium where both buoyancy forces act in the same or reverse directions has been reviewed in the literature. Boričić *et*

* Corresponding author, e-mail: mouradw002@gmail.com

al. [6], analyzed numerically an unsteady 2-D dynamic, thermal and diffusion MHD laminar boundary-layer flow over a horizontal circular cylinder of incompressible and electrical conductivity fluid with effects of thermal radiation, in a porous medium with a heat source, and chemical reactions. Lee and Hyun [7] studied numerically the double diffusion convection of an unstable flow in a rectangular cavity for the helping and opposing cases, their results were compared to other experimental results. The mixed convective heat transfer inside a ventilated cavity partially heated has been investigated by Doghmi *et al.* [8]. It was found that the flow structures and temperature distribution are considerably affected by the interaction between the inertia and the buoyancy forces. The mixed convection has been installed rapidly for small heating surfaces. Bejan and Khair [9] are interested in natural convection near a vertical surface with a porous medium. Lai and Kulacki [10] treated the same problem as Bejan and Khair [9] by analyzing the effects of injecting fluid into the wall. A detailed hydro-magnetic and thermal study of natural convection in a permeable wall with constant heat flow was carried out by Chamkha and Khaled [11]. Kamotani *et al.* [12] proposed an experimental study of natural convection in relatively long cavities with horizontal gradients of temperature and concentration.

Later, many experimental researchers have studied thermo-solutal convection in rectangular enclosures. Thevenin and Sadaoui [13] have presented numerically the steady viscous flow and heat transfer over a circular cylinder embedded in porous a medium. Thejaraju *et al.* [14], examined numerically the thermo-hydraulic performance of the louvered winglet tape inside the tube section of the double pipe heat exchanger. In order to study the thermal characteristics, the louvered winglet tape has already been discussed with the slope angle of 50, 100, 150, and 210. Their results show a satisfactory performance of louvered winglet tape over the smooth tube with a similar trend of friction factor, Nusselt number, and thermo-hydraulic performance index.

The method of submerged limits imposed on the limits was developed by Ren *et al.* [15] to simulate heat and fluid-flow across a stationary cylinder. The heat source/sink is introduced into the energy equation to analyze the immersed boundary effects. The effect of thermal boundary on the flow structure has been studied for different values of velocity and temperature. They proposed two ways to calculate the Nusselt number average by using the temperature correction at Eulerian points and the boundary heat flux at Lagrangian points. Their results show that the average Nusselt number strongly depends on Rayleigh number and aspect ratio (AR). Sayehvand *et al.* [16], examined forced convection heat transfer from two tandem circular cylinders embedded in a porous medium. Their results show that the porous medium increases the overall heat absorbed from two cylinders and cooling effect but increases the pressure drop, significantly. Hu *et al.* [17] analyzed natural convection in a square enclosure with a cylinder covered by a porous layer. Lattice Boltzmann method is used to treat the complicated interface conditions, in the case of a single domain. The curved velocity and thermal boundary conditions are treated using immersed boundary method. Their numerical results indicate that the presence of a porous layer with high thermal conductivity can greatly improve heat transfer. At low Rayleigh number (Ra = 10^3, 10^4), this investigation revealed that the porous layer has a slight influence on heat transfer. However, at high Rayleigh number, Nusselt number increases sharply with increasing Rayleigh number. The average Nusselt number increases with Darcy number and when $10^{-5} \leq \mathrm{Da} \leq 10^{-2}$, the effect of Darcy's number becomes more remarkable.

Other experimental studies in addition to these numerical studies were carried out. We can cite the study of Al-Salem *et al.* [18] in which they are interested in the thermal impact of wrapping an aluminum porous sheet over a circular tube in a heat convection configuration. The influences of porosity and thickness of the porous layer on heat transfer enhancement were investigated. Their results indicated that heat transfer is greatly enhanced with the addition of the porous layer. We notice that most of the works already cited only considered the forced convection flow. We note that relatively fewer studies focusing on natural convection using a porous ring. The simulation tests were performed for turbulent flow with varying Reynolds numbers in the range 4000 to 50000. The numerical and experimental results presented in this study demonstrate some improvements in heat transfer rate as there is a decrease in pitch to smooth tube diameter ratio, p/d, and it also increases the value of friction factor. Saada *et al.* [19] studied flow structure and heat transfer by natural convection around a porous-coated horizontal cylinder using the Darcy-Brinkmann model. It should be noted that the effects of some important parameters such as Rayleigh number and porosity were not analyzed enough.

In recent years, a study of the double-diffusive phenomenon in a porous medium has been mainly restricted to square and rectangular enclosures. The annulus geometry was studied in a few cases. Moderres *et al.* [20], investigated numerically double-diffusive convection within a 3-D in a horizontal annulus partially filled with a fluid-saturated porous medium. In their study, the average Nusselt and Sherwood numbers were presented as a function of the Lewis number, thermal Grashof number, and buoyancy ratio. Khemici *et al.* [21], carried out numerical investigations about the 3-D laminar mixed convection between two concentric horizontal cylinders. They found that cross-flow was always the main cause of the circumferential variation in fluid temperature. Also, it was noticed that the vortices obtained lead to an improvement in the heat transfer which is explained by the increase in the Nusselt number.

In this work, we present a similar study of double-diffusive natural convection through a horizontal concentric annulus between a square outer cylinder and a circular inner cylinder covered by a porous layer. This work is motivated by reason, so the main objective of this paper is to study double-diffusive natural convection through a horizontal concentric annulus between a square outer cylinder and a circular inner cylinder covered by a porous layer. Two different boundary conditions are considered: aiding and opposing buoyancy forces through both top and bottom walls.

Mathematical formulation

Problem description

The physical model is represented schematically in fig. 1. The study concerns a 2-D double-diffusive natural convection in a horizontal concentric annulus between a square outer cavity of height, L, and a circular inner cylinder of radius, r, covered by a porous layer.

Two different boundary conditions are considered. In the first case, the bottom wall has a hot temperature, T_h, and mass C_h. However, the other walls are kept at a cool temperature T_c and mass C_c. While for the second case, the bottom wall of the square outer cavity has a hot temperature, T_h, and the upper wall is kept at C_h. Though, the rest of the walls are maintained at a cool temperature T_c and mass C_c. The thermal flow continuity condition is considered on the surface of the solid cylinder. Inside the inner cylinder, there is no solutal diffusion.

To describe the flow in both fluid and porous zones, the Darcy-Brinkmann-Forchheimer model was used. In addition, the following assumptions were adopted:

– The inner cylinder is covered by a homogeneous and isotropic porous matrix with uniform porosity and tortuosity.

– All thermophysical properties of the fluid are considered to be constant.
– The solid phase temperature and that of the fluid phase are equal, local thermal equilibrium.

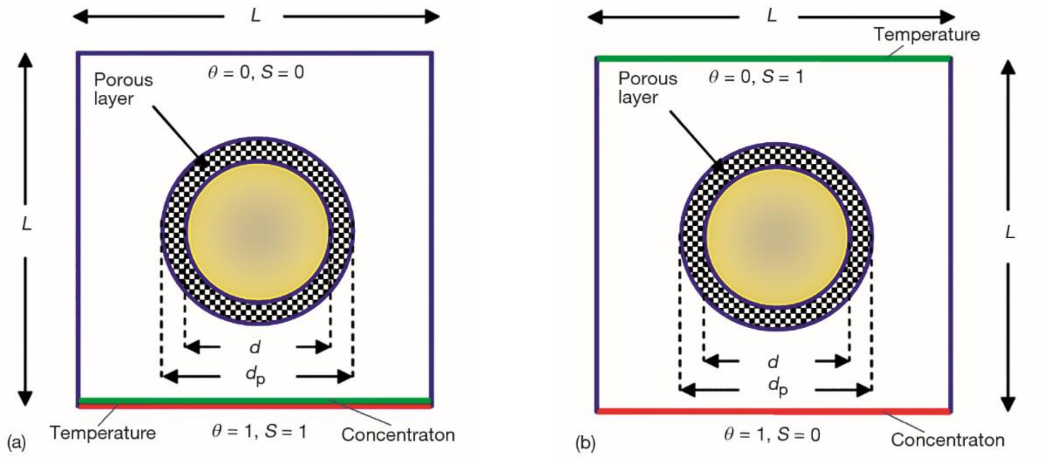

Figure 1. Schematic diagram of the problem

Governing equations

Flow is considered to be 2-D, steady, laminar, and the fluid is incompressible. In order to simplify the analysis, the Boussinesq approximation is used in a preferred variant the buoyancy terms.

Dimensionless variables are introduced in the governing equations:

$$X=\frac{x}{H},\ Y=\frac{x}{H},U=\frac{u}{\dfrac{\alpha}{H}},V=\frac{v}{\dfrac{\alpha}{H}},P=\varepsilon^2\frac{p}{\rho\left(\dfrac{\alpha}{H}\right)^2},\theta=\frac{T-T_\mathrm{c}}{T_\mathrm{h}-T_\mathrm{c}},S=\frac{C-C_\mathrm{c}}{C_\mathrm{h}-C_\mathrm{c}} \tag{1}$$

Then, the dimensionless governing equations for this problem can be written:

– Continuity:

$$\frac{\partial U}{\partial X}+\frac{\partial U}{\partial Y}=0 \tag{2}$$

– *X* momentum:

$$U\frac{\partial U}{\partial X}+V\frac{\partial U}{\partial Y}=-\nabla P+\mathrm{Pr}\,C_1\nabla^2 U-C_2\left(\varepsilon^2\frac{\mathrm{Pr}}{\mathrm{Da}}U+\varepsilon^2\frac{C_\mathrm{F}}{\sqrt{\mathrm{Da}}}\left|\vec{\mathrm{V}}\right|U\right) \tag{3}$$

– *Y* momentum:

$$U\frac{\partial V}{\partial X}+V\frac{\partial V}{\partial Y}=-\nabla P+C_1\,\mathrm{Pr}\nabla^2 V+\mathrm{Ra_T}\,\mathrm{Pr}\left(\theta+NS\right)-C_2\left(\varepsilon^2\frac{\mathrm{Pr}}{\mathrm{Da}}V+\varepsilon^2\frac{C_\mathrm{F}}{\sqrt{\mathrm{Da}}}\left|\vec{\mathrm{V}}\right|V\right) \tag{4}$$

– Energy:

$$U\frac{\partial\theta}{\partial X}+V\frac{\partial\theta}{\partial Y}=R_\lambda\nabla^2\theta \tag{5}$$

– Concentration:

$$U\frac{\partial S}{\partial X}+V\frac{\partial S}{\partial Y}=R_\mathrm{D}\nabla^2 S \tag{6}$$

The dimensionless parameters governing double-diffusive natural convection in the porous annulus are thermal Rayleigh number, $\mathrm{Ra_T}$, the Darcy number, Da, the Prandtl number, Pr, the Lewis number, Le, the Buoyancy ratio, N, kinematic viscosity ratio, R_μ, mass diffusivity ratio, R_D, thermal conductivity ratio, R_λ, and the Forchheimer coefficient, C_F, defined by:

$$\mathrm{Ra_T}=\frac{\mathrm{g}\beta_\mathrm{T}L^3(T_\mathrm{h}-T_\mathrm{c})}{\nu^2},\ \mathrm{Da}=\frac{k}{H^2},\ \mathrm{Pr}=\frac{\gamma}{\alpha},\ \mathrm{Le}=\frac{\alpha}{D},\ N=\frac{\beta_\mathrm{S}\Delta C}{\beta_\mathrm{T}\Delta T},\ R_\mu=\frac{\mu_\mathrm{eff}}{\mu},$$

$$R_\mathrm{D}=\frac{D_\mathrm{eff}}{D},\ R_\lambda=\frac{\lambda_\mathrm{eff}}{\lambda},\ \left|\vec{\mathrm{V}}\right|=\sqrt{U^2+V^2},\ C_\mathrm{F}=\frac{1.75}{\sqrt{150\,\varepsilon^3}} \tag{7}$$

If R_μ, R_λ, R_D, and C_1 are equal to 1 and C_2 equals to 0, the medium is fluid, and if $C_1 = \varepsilon R_\mu$, $C_2 = 1$ the medium is a porous layer, although to inside the inner cylinder we take $R_\lambda = 0.025$ and $R_\mu = \infty$.

In addition to the above dimensionless parameters, the present study also involves the geometrical parameters, such as the *AR*, given by: $AR = L/d$.

The dimensionless boundary conditions are:
– Inside the cylinder: $U = 0$, $V = 0$, $S = 0$.
– On the surface of the solid cylinder: $\nabla\theta_\mathrm{s}=R_\mathrm{s}\nabla\theta_\mathrm{eff}$.
– External boundary conditions.
  • The first case (aiding buoyancy forces):

$$\begin{aligned}
&U=0,\quad V=0,\quad \theta=1,\quad S=1\quad \text{for}\quad Y=0,\quad 0\le X\le 1\\
&U=0,\quad V=0,\quad \theta=0,\quad S=0\quad \text{for}\quad Y=1,\quad 0\le X\le 1\\
&U=0,\quad V=0,\quad \theta=0,\quad S=0\quad \text{for}\quad X=0,\quad 0\le Y\le 1\\
&U=0,\quad V=0,\quad \theta=0,\quad S=0\quad \text{for}\quad X=1,\quad 0\le Y\le 1
\end{aligned} \tag{8}$$

  • The second case (opposing buoyancy forces):

$$\begin{aligned}
&U=0,\quad V=0,\quad \theta=1,\quad S=0\quad \text{for}\quad Y=0,\quad 0\le X\le 1\\
&U=0,\quad V=0,\quad \theta=0,\quad S=1\quad \text{for}\quad Y=1,\quad 0\le X\le 1\\
&U=0,\quad V=0,\quad \theta=0,\quad S=0\quad \text{for}\quad X=0,\quad 0\le Y\le 1\\
&U=0,\quad V=0,\quad \theta=0,\quad S=0\quad \text{for}\quad X=1,\quad 0\le Y\le 1
\end{aligned} \tag{9}$$

Heat and mass transfers through the cavity are characterized by the Nusselt and Sherwood numbers. Since the active walls (horizontal walls) are subjected to constant temperatures and concentrations, the locale values of heat and mass transfers at a position x are written:

$$\mathrm{Nu}=-\left.\frac{\partial\theta}{\partial Y}\right|_{Y=0},\ \mathrm{Sh}=-\left.\frac{\partial S}{\partial Y}\right|_{Y=0\ \text{or}\ Y=1} \tag{10}$$

The average Nusselt and average Sherwood numbers can be defined:

$$\overline{\mathrm{Nu}} = -\frac{1}{L}\int_0^L \left(\frac{\partial \theta}{\partial Y}\right)\mathrm{d}X \ , \ \overline{\mathrm{Sh}} = -\frac{1}{L}\int_0^L \left(\frac{\partial S}{\partial Y}\right)\mathrm{d}X \tag{11}$$

Finally, the dimensionless stream function, ψ, is calculated by integrating the dimensionless velocity:

$$U = \frac{\partial \psi}{\partial Y} \ , \ V = -\frac{\partial \psi}{\partial X} \tag{12}$$

Numerical procedure

The finite volume method used in the present study was described by Patankar [22]. The combined continuity, momentum, energy, and concentration equations have been solved numerically using the SIMPLE algorithm. These equations can be written in a general transport equation as:

$$\frac{\partial(\rho U \phi)}{\partial X} + \frac{\partial(\rho U \phi)}{\partial Y} = \frac{\partial}{\partial X}\left[\Gamma_\phi\left(\frac{\partial \phi}{\partial X}\right)\right] + \frac{\partial}{\partial Y}\left[\Gamma_\phi\left(\frac{\partial \phi}{\partial Y}\right)\right] + S_\phi \tag{13}$$

This equation serves as a starting point for a computational procedure in (FVM) Ferziger and Peric [23]. Effect of mesh size on the streamlines, isotherms, and iso-concentrations is studied. We note that the flow structure is obtained in its final form which no longer varies for a mesh of (302 × 302), fig. 2. Consequently, all our simulations will be executed with this mesh. Figure 3, shows the effect of the mesh density on the current lines, the isotherms, and the iso-concentrations in the case where the horizontal walls are maintained at constant temperatures and concentrations.

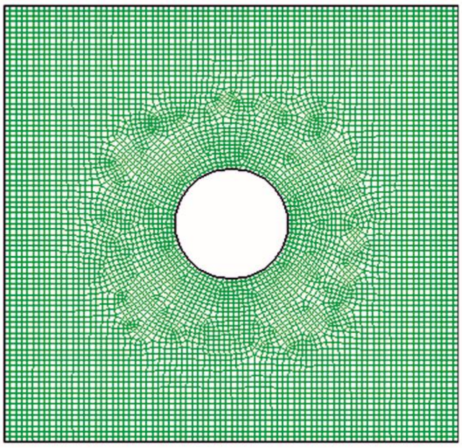

Figure 2. Mesh distribution inside the simulated geometry

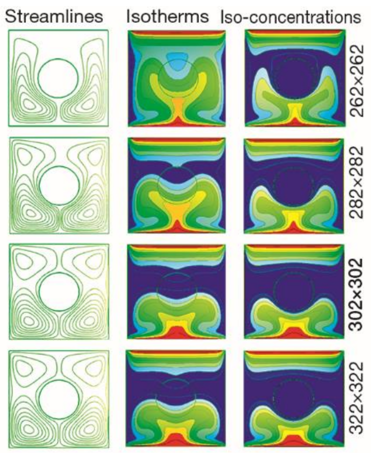

Figure 3. Effect of grid size on the streamlines, isotherms, and iso-concentrations for: Da = 10^{-3}, $\mathrm{Ra_T} = 10^6$, $\mathrm{Ra_s} = 10^5$

A simple, 2-D, and square mesh is used. Thus, to obtain accurate results, we need very fine grids near the walls and at the interface between fluid and porous matrix, where the velocity, concentration, and temperature gradients are large compared to other regions. The iteration method used in this program is a line-by-line procedure, which is a combination of the direct method and the resulting tridiagonal matrix algorithm. The accuracy was defined by the change in the average Nusselt number and the other dependent variables through one hundred iterations to be less than 0.02% from its value. The check showed that 3500 iterations were enough for all of the study values.

Code validation

The numerical technique implemented in the present developed code study has been successfully employed in our recent papers to investigate the effects of several parameters on heat and mass transfer. However, to verify the accuracy of the current numerical results, simulations of the present model are tested and compared with different reference solutions available in the literature for natural double-diffusive convection in a porous annulus. The program was run when the dimensionless temperature at the outer square cavity was kept constant and his value equal one, while his value at the inner cylinder equal zero. These conditions were the same as those studied by Hu *et al.* [17], fig. 4.

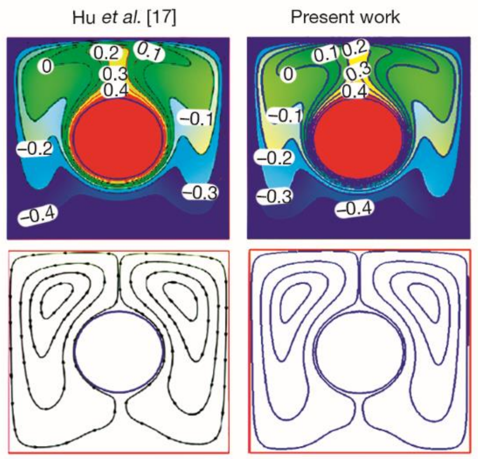

Figure 4. Comparisons of the streamlines and isotherms between the present work and that of, Hu *et al.* [17], case without porous medium for Ra = 10^6

Results and discussion

In this section, the numerical results for double-diffusive natural convection in a horizontal concentric annulus between a square outer cavity and a circular inner cylinder partially or completely filled with a porous medium are presented and discussed. The non-dimensional controlling parameters for this investigation are the Darcy number, thermal conductivity ratio, R_λ, aspect ratio, AR, thermal Rayleigh number, $\mathrm{Ra_T}$, and the Buoyancy ratio, N. In the present paper, the thermal Rayleigh number, thermal conductivity ratio, and the Buoyancy ratio are, respectively, varied in the ranges $10^4 \le \mathrm{Ra_T} \le 10^8$, $-100 \le N \le 100$ to over both aiding and opposing cases. Three representative cases with AR = 1.667, 2.5, 5 are simulated. In the following sections, the flow fields, temperature, and concentration distributions in the fluid and porous annulus are illustrated through streamlines, isotherms, and iso-concentrations.

Effect of the buoyancy ratio number

In the double-diffusive convection system, the buoyancy forces can aid or oppose the fluid-flow. In the present investigation, we have studied both aiding and opposing buoyancy forces effects on the structure of the fluid-flow. Figures 5 and 6, show the numerical results visualized through the streamlines, isotherms, and iso-concentrations. The values of the buoyancy forces ratio applied to the upper and lower walls of the square cavity are $N = \pm 1, \pm 10, \pm 50, \pm 100$. The annulus cavity is completely filled with a porous medium. As is shown clearly in figs. 5 and 6, streamlines, isotherms, and iso-concentrations are symmetrical about the vertical axis of the annulus, because there is a symmetry of geometry conditions. This symmetry exists also about the horizontal axis to the streamlines in the case where N = –1

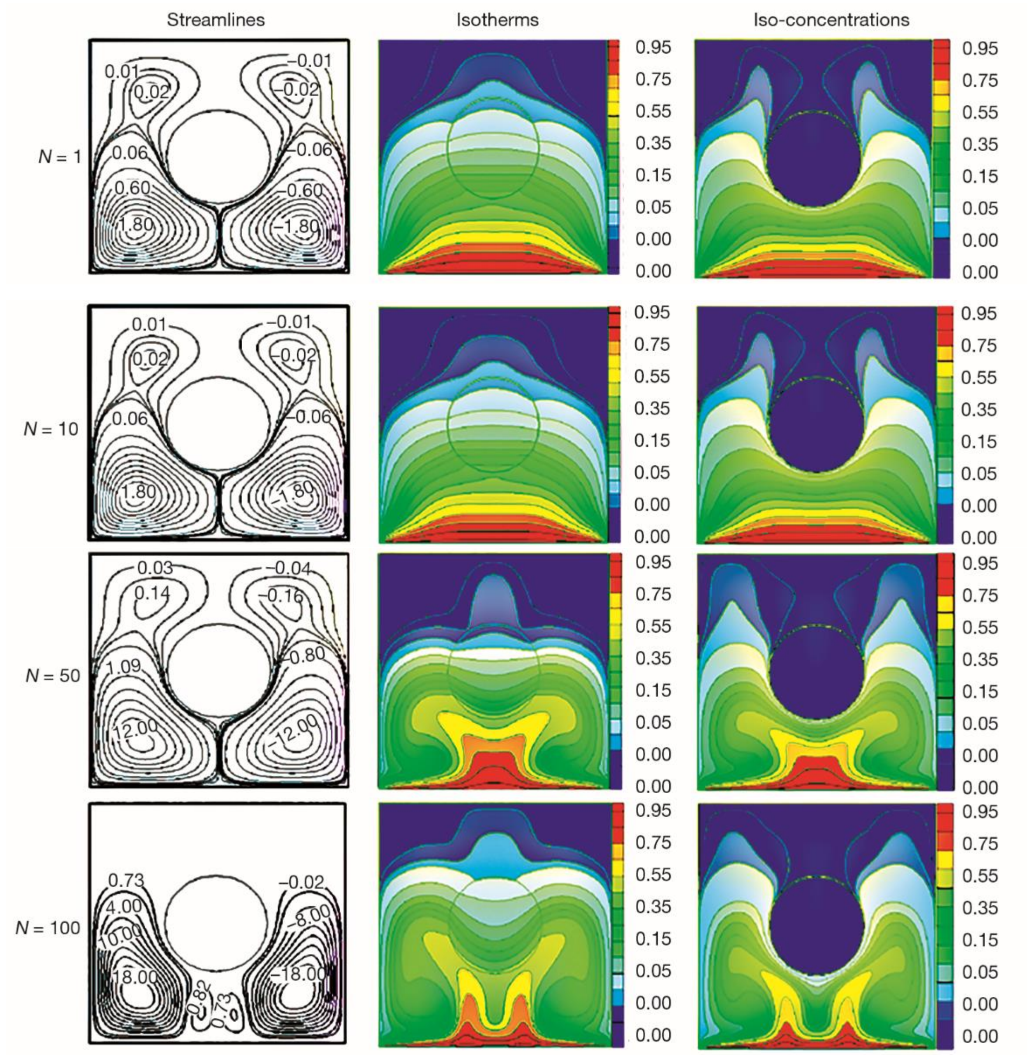

Figure 5. Streamlines, isotherms, and iso-concentrations for different values of buoyancy ratio number for aiding case, when $Ra_s = 10^5$, $Da = 10^{-3}$, $Pr = 0.71$, $Sc = 0.67$, $\varepsilon = 0.4$, and $R_\alpha = 10$

(symmetry of boundary conditions). For positive values of the buoyancy ratio, N, visualized in fig. 5, and for low values of N, the dynamic processes of natural convection show that they are four eddies of different sizes firstly are originated in the annulus cavity, two big eddies below the horizontal axis and two small located above the same axis. When N increases from 1 to 100, two small eddies were appeared between the two big original eddies. Because of the buoyancy effect and the thermal boundary-layer on the bottom surface of the cavity more than that on its top surface. The buoyancy ratio, N, affects significantly the heat and mass transfer characteristics, a consequence of this, the thermal and solutal boundary-layer near the heated surface are very thick. For the opposing case, when the buoyancy forces are applied in inverse directions, it is found four eddies of the same sizes. However, as the buoyancy ratio is increasing, the sizes of the two upper vortices decreases then each original eddy will split into two small eddies until they finally disappear at $N = 100$. We note also that when the absolute value of buoyancy ratio increases in figs. 5 and 6, the isotherms and iso-concentrations are strongly distorted and disordered, which means that the effect of convection increases strongly. It denotes that the flow in the annulus is mainly dominated by convection.

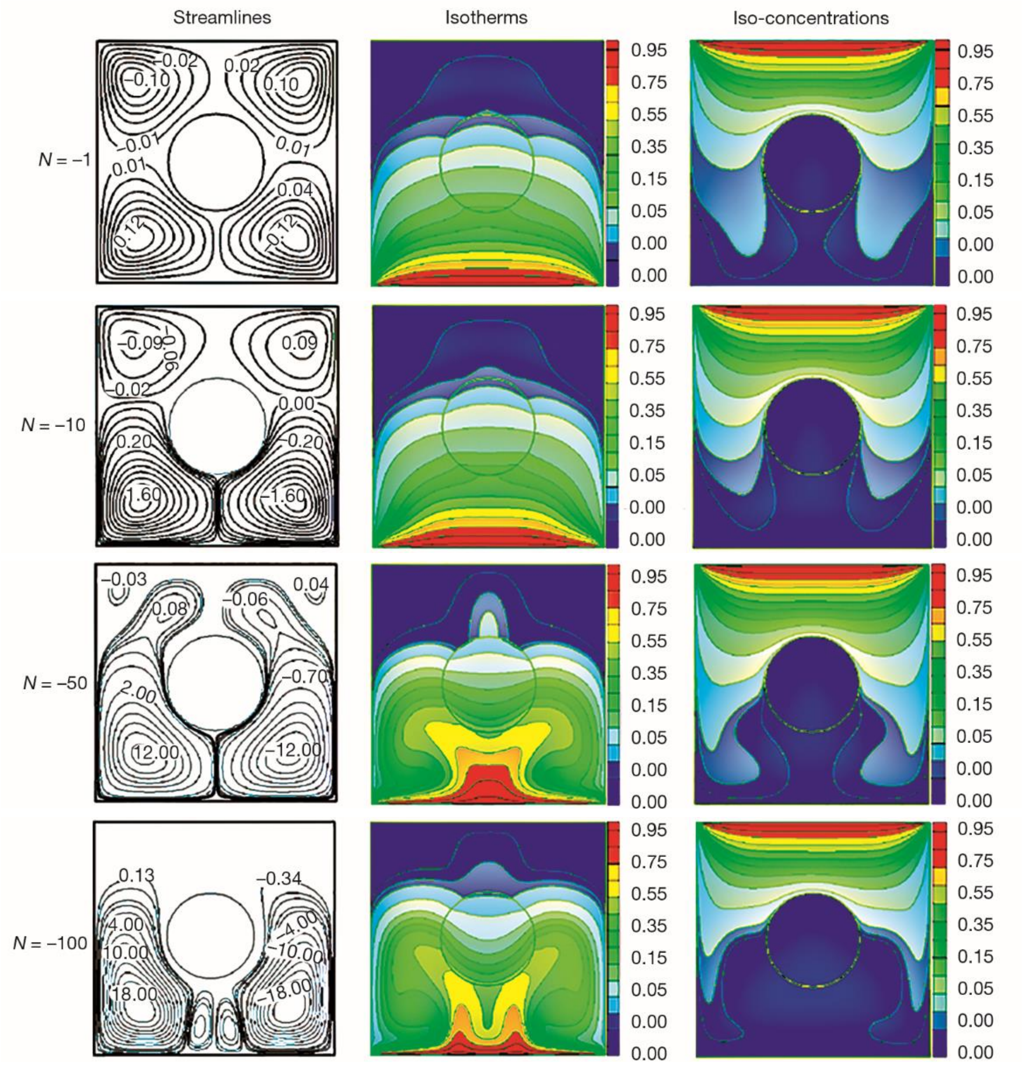

Figure 6. Streamlines, isotherms, and iso-concentrations for different values of buoyancy ratio number for opposing case, when $\mathrm{Ra_s} = 10^5$, $\mathrm{Da} = 10^{-3}$, $\mathrm{Pr_c} = 0.71$, $\mathrm{Sc} = 0.67$, $\varepsilon = 0.4$, and $R_\alpha = 10$

Effect of thermal Rayleigh number and thermal diffusivity ratio

Figure 7 reveals the influence of the thermal diffusivity ratio and thermal Rayleigh number on the average values of Nusselt and Sherwood numbers along the heated surface.

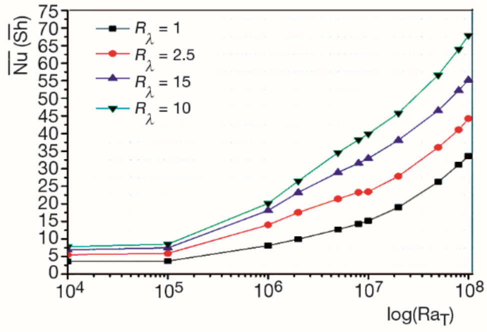

Figure 7. Effect of the thermal Rayleigh number on the $\overline{\mathrm{Nu}}$ ($\overline{\mathrm{Sh}}$) for different values of thermal diffusivity ratio, Da = 10^{-3}, Pr = 0.71, Sc = 0.67, ε = 0.4, and R_α = 10

The values of thermal Rayleigh number for this simultaneous are varied from 10^4 to 10^8 when ε = 0.7. It is found that both average Nusselt and Sherwood numbers increase with increasing the thermal diffusivity ratio and thermal Rayleigh number. Save that, when $\mathrm{Ra_T}$ varies between 10^4 and 10^5, we note that $\overline{\mathrm{Nu}}$ and $\overline{\mathrm{Sh}}$ are little affected by $\mathrm{Ra_T}$ number for all values of R_λ. However, at high values of thermal Rayleigh number ($\mathrm{Ra_T} > 10^5$), it can be observed that $\overline{\mathrm{Nu}}$ and $\overline{\mathrm{Sh}}$ increase sharply. The increase of thermal diffusivity ratio causes higher fluid re-circulation in the annular space due to the gradient in density, and consequently, the Nusselt and Sherwood numbers increase with increasing thermal diffusivity ratio. To have a better understanding of the heat and mass transfer in this system, we also studied the effect of thermal Rayleigh number on the temperature and concentration profiles for three positions inside the cavity: Y = 0.15, Y = 0.5, and Y = 0.85, fig. 8. We considered the variation of the temperature inside the cylinder and the annulus space is partially filled with porous medium. For the section located above the internal cylinder, it is clear that the temperature and concentration profiles decrease by increasing the thermal Rayleigh number, due to the greater heat-inducing strong buoyant flow in this region of an annulus. However, an increase in $\mathrm{Ra_T}$ implies the enhancement in temperature and concentration values in the mid-section. Inside the inner cylinder, it is observed two behaviors of temperature profiles. In fact, at low thermal Rayleigh number $(\mathrm{Ra_T} \leq 10^6)$, the temperature profiles are parabolic upward, therefore the cylinder becomes like a heat source. However, when $\mathrm{Ra_T} \geq 2 \cdot 10^6$, the profiles are the same shape but are directed downward, which means that the heat transfer occurs from the interface to the cylinder center. At $\mathrm{Ra_T} = 1.5 \cdot 10^6$, the profile is almost linear. Conversely, a shift in both temperature and concentration can be observed at Y = 0.15 compared with the case at Y = 0.5. In this latter case, we observed that for large values of thermal Rayleigh number the heat spreads more in the central region of this section.

Conclusions

Natural convection heat and mass transfer in an annulus partially filled with a fluid-saturated porous medium, between the outer cavity and the inner cylinder are investigated numerically for different conditions of temperature and concentration, as well as different values of the buoyancy ratio. The results obtained are compared with each other and are checked against those of other authors for similar cases. A good agreement is found in particular for the streamlines and isotherms, as well as for the average Nusselt and Sherwood numbers. The most important results obtained can be presented as follows.

- The buoyancy ratio has a significant effect on the flow structure and also on the thermal and solutal fields. As a consequence of this, the thermal and solutal boundary-layers near the heated surface are very thick.
- Both average Nusselt and Sherwood numbers increase with increasing the thermal diffusivity ratio and thermal Rayleigh number. However, when $\mathrm{Ra_T}$ varies between 10^4 and 10^5, it is found that $\overline{\mathrm{Nu}}$ and $\overline{\mathrm{Sh}}$ are weakly affected by Ra_T number for all values of R_λ.

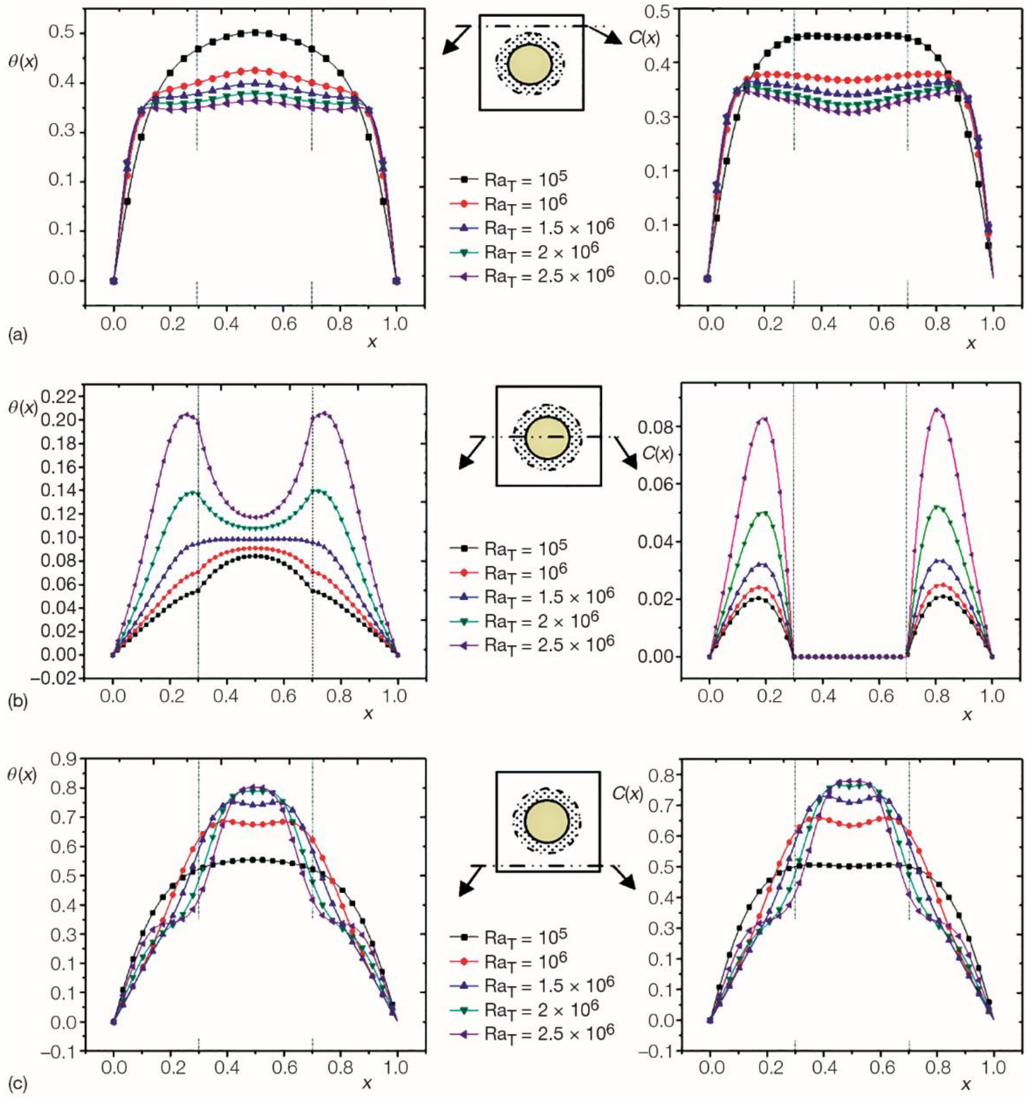

Figure 8. Effect of the thermal Rayleigh number on the temperature and concentration profiles through three sections; (a) Y = 0.85, (b) Y = 0.50, and (c) Y = 0.15, for Da = 10^{-3}, Pr = 0.71, Sc = 0.67, ε = 0.4, and R_α = 1

- The temperature and concentration profiles decrease about 34.56% by increasing the thermal Rayleigh number, in the section located above the internal cylinder, due to the greater heat-inducing strong buoyant flow in this region of an annulus.
- An increase in Ra_T number implies a sharp increase in temperature and concentration values in the mid-section. Inside the inner cylinder, it is observed two different behaviors of temperature profiles. At low values of Ra_T number, the evaluation of the temperature shows that the cylinder becomes a heat source since its temperature is high compared to the temperature of interfaces. The opposite situation was observed for high values of Ra_T.

Acknowledgment

This research was supported by the Ministry of Higher Education and Scientific Research of Algeria through collaboration between the laboratory FIMA of UDBKM in Algeria and Interdisciplinary Laboratory Carnot of Bourgogne ICB UMR 6303 of UTBM Belfort France.

Nomenclature

AR – aspect ratio, (= L/d)
C – concentration, [kgm^3]
C_F – Forchheimer coefficient
D – mass diffusivity, [m^{2}s^{-1}]
Da – Darcy number, (= k/H^2)
d – inner cylinder diameter, [m]
d_p – porous layer diameter, [m]
g – gravitational acceleration, [ms^{-2}]
k – permeability of the porous medium, [m^2]
L – side length of the square outer cylinder, [m]
Le – Lewis number, (= Sc/Pr)
N – buoyancy ratio number, (= $\mathrm{Ra_s/Ra_T}$)
Nu – local Nusselt number, $\left[= -\left.\dfrac{\partial\theta}{\partial Y}\right|_{Y=0}\right]$
$\overline{\mathrm{Nu}}$ – average Nusselt number, $\left[= -\dfrac{1}{L}\int_0^L \left(\dfrac{\partial\theta}{\partial Y}\right)\mathrm{d}X\right]$
P – dimensionless pressure
p – pressure, [Nm^{-2}]
Pr – Prandtl number,[$= \gamma/\alpha$]
$\mathrm{Ra_s}$ – Solutal Rayleigh number based on the gap width, $\left[= \dfrac{\mathrm{g}\beta_S L^3(C_\mathrm{h} - C_\mathrm{c})}{\nu^2}\right]$
$\mathrm{Ra_T}$ – thermal Rayleigh number based on the gap width, $\left[= \dfrac{\mathrm{g}\beta_T L^3(T_\mathrm{h} - T_\mathrm{c})}{\nu^2}\right]$
R_D – ratio of solutal diffusivity, $(= D_\mathrm{eff}/D)$
R_s – ratio of thermal conductivity porous/solid, (= $\lambda_\mathrm{eff}/\lambda_\mathrm{s}$)
R – inner cylinder radius $(=[(X-0.5)^2 + (Y-0.5)^2]^{1/2})$
R_λ – ratio of thermal conductivity porous/fluid, $[= \lambda_\mathrm{eff}/\lambda_\mathrm{f}]$
R_μ – viscosity ratio, $[= \mu_\mathrm{eff}/\mu]$
S – dimensionless concentration, [= $(C - C_c)/(C_\mathrm{h} - C_c)$]
S_ϕ – linearized source term for ϕ
$\overline{\mathrm{Sh}}$ – average Sherwood number, $\left[= -1/L\int_0^L (\partial S/\partial Y)\mathrm{d}X\right]$
Sc – Schmidt number, $(= \gamma/\mathrm{D})$
Sh – local Sherwood number, $\left(= -\left.\dfrac{\partial S}{\partial Y}\right|_{Y=0}\right)$
T – local temperature, [K]
T_h, T_c – temperature of hot and cool walls, respectively, [K]
ΔT – temperature difference, (= $T_\mathrm{h} - T\mathrm{c}$), [K]
U, V – dimensionless velocity components in x and y directions
u, v – velocity components along x- and y-directions, respectively
x, y – cartesian co-ordinate in horizontal and vertical directions respectively, [m]
X, Y – dimensionless co-ordinate in horizontal and vertical directions respectively

Greek symbols

λ – thermal conductivity, [Wm^{2}K^{-1}]
α – thermal diffusivity, [m^{2}s^{-1}]
β_S – solutal expansion coefficient, [m^{3}kg^{-1}]
β_T – thermal expansion coefficient, [mK^{-1}]
Γ_ϕ – diffusion coefficient for parameter ϕ
ε – porosity
θ – dimensionless temperature, [= $(T - T_c)/(T_\mathrm{h} - T_c)$]
ρ – density, [Kgm^{-3}]
ν – kinematic viscosity, [m^{2}s^{-1}]
ψ – stream function

Subscripts

h – hot
c – cold
eff – effective
s – solid

References

[1] Combarnous, M., Bories, S., Hydrothermal Convection in Saturated Porous Media, *Advances in hydroscience*, *10* (1975), pp. 231-307

[2] Nield, D. A., Bejan, A., *Convection in porous media*, Springer, New York, USA, 2006
[3] Valipour, M. S., *et al.*, Magnetohydrodynamics Flow and Heat Transfer Around a Solid Cylinder Wrapped with a Porous Ring, *Journal of Heat Transfer*, *136* (2014), 6, 062601
[4] Yang, M., Ma, N., Free Convection in a Liquid-Encapsulated Molten Semiconductor in a Vertical Magnetic Field, *International Journal of Heat and Mass Transfer*, *48* (2005), 19, pp. 4010-4018
[5] Vijaya Venkata Raman, S., *et al.*, A Review of Solar Drying Technologies, *Renewable and sustainable energy reviews*, *16* (2012), 5, pp. 2652-2670
[6] Boričić, A. Z., *et al.*, MHD Effects on Unstedy Dynamic, Thermal and Diffusion Boundary-layer Flow Over a Horizontal Circular Cylinder, *Thermal Science*, *16* (2012), Suppl. 2, pp. S311-S321
[7] Lee, J. W., Hyun, J. M., Double-Diffusive Convection in a Rectangle with Opposing Horizontal Temperature and Concentration Gradients, *International Journal of Heat and Mass Transfer*, *33* (1990), 8, pp. 1619-1632
[8] Doghmi, H., *et al.*, Three-Dimensional Mixed Convection Heat Transfer in a Partially Heated Ventilated Cavity, *Thermal Science*, *24* (2020), 3B, pp. 1895-1907
[9] Bejan, A., Khair, K. R., Heat and Mass Transfer by Natural Convection in a Porous Medium, *International Journal of Heat and Mass Transfer*, *28* (1985), 5, pp. 909-918
[10] Lai, F., Kulacki, F., Non-Darcy Mixed Convection Along a Vertical Wall in a Saturated Porous Medium, *Journal of Heat Transfer*, *113* (1991), 1, pp. 252-255
[11] Chamkha, A. J., Khaled, A. R. A., Hydromagnetic Coupled Heat and Mass Transfer by Natural Convection from a Permeable Constant Heat Flux Surface in Porous Media, *Journal of Porous Media*, *3* (2000), 3, pp. 259-266
[12] Kamotani, Y., *et al.*, Experimental Study of Natural Convection in Shallow Enclosures with Horizontal Temperature and Concentration Gradients, *International Journal of Heat and Mass Transfer*, *28* (1985), 1, pp. 165-173
[13] Thevenin, J., Sadaoui, D., About Enhancement of Heat Transfer Over a Circular Cylinder Embedded in a Porous Medium, *International Communications in Heat and Mass Transfer*, *22* (1995), 2, pp. 295-304
[14] Thejaraju, R., *et al.*, Numerical Evaluation of Thermo-Hydraulic Performance Index of a Double Pipe Heat Exchanger Using Double Sided Louvered Winglet Tape, *Journal of Thermal Engineering*, *6* (2020), 5, pp. 843-857
[15] Ren, W., *et al.*, Boundary Condition-Enforced Immersed Boundary Method for Thermal Flow Problems with Dirichlet Temperature Condition and Its Applications, *Computers & Fluids*, *57* (2012), Mar., pp. 40-51
[16] Sayehvand, H. O., *et al.*, Numerical Analysis of Forced Convection Heat Transfer from Two Tandem Circular Cylinders Embedded in a Porous Medium, *Thermal Science*, *21* (2017), 5, pp. 2117-2128
[17] Hu, Y., *et al.*, Immersed Boundary-Lattice Boltzmann Simulation of Natural Convection in a Square Enclosure with a Cylinder Covered by Porous Layer, *International Journal of Heat and Mass Transfer*, *92* (2016), Jan., pp. 1166-1170
[18] Al-Salem, K., *et al.*, Effects of Porosity and Thickness of Porous Sheets on Heat Transfer Enhancement in a Cross Flow Over Heated Cylinder, *International Communications in Heat and Mass Transfer*, *38* (2011), 9, pp. 1279-1282
[19] Saada, M. A., *et al.*, Natural Convection Around a Horizontal Solid Cylinder Wrapped with a Layer of Fibrous or Porous Material, *International Journal of Heat and Fluid-flow*, *28* (2007), 3, pp. 483-495
[20] Moderres, M., *et al.*, Numerical Investigation of Double-Diffusive Mixed Convection in Horizontal Annulus Partially Filled with a Porous Medium, *International Journal of Numerical Methods for Heat & Fluid-flow*, *27* (2017), 4, pp. 773-794
[21] Khemici, M., *et al.*, Numerical Study of Developing Laminar Mixed Convection in a Heated Annular Duct with Temperature Dependent Properties, *Thermal Science*, *23* (2019), 6A, pp. 3411-3423
[22] Patankar, S., *Numerical heat transfer and fluid-flow*, CRC press, Boka Raton, Fla., USA, 1980
[23] Ferziger, J. H., Peric, M., *Computational Methods for Fluid Dynamics*, Springer Science & Business Media, New York, USA, 2012

Paper submitted: February 15, 2021
Paper revised: April 19, 2021
Paper accepted: April 21, 2021